THE JOURNAL OF BIOLOGICAL CHEMISTRY VOL. 287, NO. 50, pp. 41861–41874, December 7, 2012


# Functional Characterization of TbMCP5, a Conserved and Essential ADP/ATP Carrier Present in the Mitochondrion of the Human Pathogen *Trypanosoma brucei*[*]

Received for publication, July 25, 2012, and in revised form, September 28, 2012 Published, JBC Papers in Press, October 16, 2012, DOI 10.1074/jbc.M112.404699

**Priscila Peña-Diaz[‡1], Ludovic Pelosi[§1], Charles Ebikeme[¶], Claudia Colasante[‖], Fei Gao[‡], Frederic Bringaud[¶], and Frank Voncken[‡2]**

*From the [‡]Department of Biological Sciences and Hull York Medical School, University of Hull, Cottingham Road, HU6 7RX Hull, United Kingdom, the [§]Université Joseph Fourier, Equipe Dynamique des Organelles et Plasticité Cellulaire, Laboratoire de Biologie à Grande Echelle, iRTSV-CEA de Grenoble, 17 Rue des Martyrs, 38054 Grenoble Cedex 9, France, the [¶]Centre de Résonance Magnétique des Systèmes Biologiques, Université Bordeaux Segalen, CNRS UMR-5536, 146 Rue Léo Saignat, 33076 Bordeaux Cedex, France, and [‖]Medizinische Zellbiologie, Institut für Anatomie und Zellbiologie II, Justus-Liebig-Universität Giessen, Aulweg 123, 35385 Giessen, Germany*

**Background:** TbMCP5 was predicted to function as a mitochondrial ADP/ATP carrier.
**Results:** TbMCP5 functionally complemented *ANC*-deficient *S. cerevisae*, has biochemical properties comparable with those of ScAnc2p, and is essential for mitochondrial ADP/ATP exchange in *T. brucei*.
**Conclusion:** TbMCP5 is a conserved and essential mitochondrial ADP/ATP carrier in *T. brucei*.
**Significance:** TbMCP5 is the first functionally characterized mitochondrial ADP/ATP carrier from a kinetoplastid parasite.

***Trypanosoma brucei* is a kinetoplastid parasite of medical and veterinary importance. Its digenetic life cycle alternates between the bloodstream form in the mammalian host and the procyclic form (PCF) in the bloodsucking insect vector, the tsetse fly. PCF trypanosomes rely in the glucose-depleted environment of the insect vector primarily on the mitochondrial oxidative phosphorylation of proline for their cellular ATP provision. We previously identified two *T. brucei* mitochondrial carrier family proteins, TbMCP5 and TbMCP15, with significant sequence similarity to functionally characterized ADP/ATP carriers from other eukaryotes. Comprehensive sequence analysis confirmed that TbMCP5 contains canonical ADP/ATP carrier sequence features, whereas they are not conserved in TbMCP15. Heterologous expression in the *ANC*-deficient yeast strain *JL1Δ2Δ3u*$^-$ revealed that only TbMCP5 was able to restore its growth on the non-fermentable carbon source lactate. Transport studies in yeast mitochondria showed that TbMCP5 has biochemical properties and ADP/ATP exchange kinetics similar to those of Anc2p, the prototypical ADP/ATP carrier of *S. cerevisiae*. Immunofluorescence microscopy and Western blot analysis confirmed that TbMCP5 is exclusively mitochondrial and is differentially expressed with 4.5-fold more TbMCP5 in the procyclic form of the parasite. Silencing of TbMCP5 expression in PCF *T. brucei* revealed that this ADP/ATP carrier is essential for parasite growth, particularly when depending on proline for energy generation. Moreover, ADP/ATP exchange in isolated *T. brucei* mitochondria was eliminated upon TbMCP5 depletion. These results confirmed that TbMCP5 functions as the main ADP/ATP carrier in the trypanosome mitochondrion. The important role of TbMCP5 in the *T. brucei* energy metabolism is further discussed.**

The Kinetoplastida are the earliest-branching unicellular eukaryotes to possess "classical" mitochondria (1). They include the closely related trypanosomatid protozoa *Trypanosoma brucei*, *Trypanosoma cruzi*, and *Leishmania* sp., which have been well studied mainly because of their significant medical and veterinary importance (see the World Health Organization Web site). *T. brucei* is predominantly found in sub-Saharan Africa, and its subspecies are the etiological agents of sleeping sickness in humans and the wasting disease "Nagana" in cattle. The complex life cycle of *T. brucei* includes two replicating forms that can be grown *in vitro*: the bloodstream form (BSF)[3] found in the blood and tissue fluids of the mammalian host and the procyclic form (PCF) in the intestinal tract and salivary glands of the bloodsucking insect vector, the tsetse fly. The energy metabolism of the parasite is subject to substantial rearrangements in order to adapt to the distinct host environments (2, 3). BSF trypanosomes rely exclusively on glucose and its degradation by glycolysis for their cellular energy (ATP) provision, with pyruvate and glycerol excreted as incomplete fermentation products. Most of the glycolytic pathway is compartmentalized in a specialized peroxisome, the glycosome (3). ATP

* This work was supported by BBSRC Grant BB/G00448X/1 (to F. V.); by grants from the University Joseph Fourier, CNRS, and the Commissariat à l'Energie Atomique et aux Energies Alternatives (programme Signalisation et Transport Membranaire) (to L. P.); and by grants METABOTRYP of the ANR-MIME2007 call and ACETOTRYP of the ANR-BLANC-2010 call from CNRS, the Université Bordeaux Segalen, the Conseil Régional d'Aquitaine, and the Agence Nationale de la Recherche (ANR) programs (to F. B.).
[1] Both authors contributed equally to this work.
[2] To whom correspondence should be addressed. Tel.: 44-1482-465280; Fax: 44-1482-465458; E-mail: F.Voncken@hull.ac.uk.

[3] The abbreviations used are: BSF, bloodstream form; PCF, procyclic form; ASCT, acetate:succinate CoA-transferase; ATR, atractyloside; N-ATR, 6′-*O*-naphthoyl-atractyloside; BA, bongkrekic acid; CATR, carboxyatractyloside; MCF, mitochondrial carrier family; N-ADP, 3′-*O*-(1-naphthoyl)-adenosine 5′-diphosphate; SCoAS, succinyl-CoA synthase; YNB, yeast nitrogen broth medium; YPL, rich yeast extract peptone lactate medium; $Ap_5A$, $P^1$,$P^5$-diadenosine-pentaphosphate; PEPCK, phosphoenolpyruvate carboxykinase.

production and consumption in the glycosome is balanced, and it has been postulated that this organelle does not provide ATP to the rest of the cell (3). Instead, net production of ATP occurs in the final and cytosolic part of the glycolytic pathway, during the conversion of phosphoenolpyruvate to pyruvate. The BSF mitochondrion lacks key enzymes and components of the Krebs cycle, and its role in the energy metabolism is restricted to the reoxidation of glycosome-derived glycerol-3-phosphate by an alternative oxidase located at the inner mitochondrial membrane (4, 5). The procyclic form of *T. brucei* has a more elaborate energy metabolism, predominantly depending on the mitochondrion (6). Remarkably, PCF trypanosomes do not use the Krebs cycle for the generation of ATP (7). Instead, ATP is mainly generated by the incomplete aerobic fermentation of glucose present in the blood meal or from proline found in the insect vector (8, 9). During glycolysis, the metabolic intermediate phosphoenolpyruvate is produced in the cytosol. Depending on the cellular redox and ATP balances, phosphoenolpyruvate is converted to pyruvate and further metabolized in the mitochondrion to acetate, or it enters the glycosome, where it is converted to succinate via the succinic fermentation branch (10). Under glucose-depleted conditions, which reflect the insect midgut environment, proline is catabolized in the mitochondrion where ATP is mainly produced from oxidative phosphorylation (9, 11). However, under glucose-rich conditions, ATP is primarily produced by substrate-level phosphorylation, whereas oxidative phosphorylation becomes essential in the absence of glucose (8–12).

The inner mitochondrial membrane of *T. brucei* is thought to be impermeable to metabolites (13), implying the presence of specific membrane-bound transporters. Mitochondrial carrier family (MCF) proteins are located in the inner mitochondrial membrane and mediate the transport of a wide range of metabolic intermediates (see Ref. 14 and references therein). As the predominant mitochondrial metabolite transporters, they exert flux control on metabolic pathways and are involved in the maintenance of cellular redox and ATP balances (14). In particular, the mitochondrial ADP/ATP carrier plays an important role in sustaining the cellular ATP homeostasis by facilitating the 1:1 counterexchange of mitochondrial ATP for cytosolic ADP (15). The evolution of the ADP/ATP carrier has been key to the evolution of the eukaryotic cell by enabling the establishment of the mitochondrion as an ATP-generating organelle. ADP/ATP carriers have been extensively and predominantly studied in a wide range of higher eukaryotes (14, 16), whereas virtually nothing is known about their homologues from earlier branching eukaryotes, such as the Kinetoplastida. We previously reported that the genome of *T. brucei* codes for 24 different MCF proteins (17). Two of the identified MCF proteins, TbMCP5 and TbMCP15, showed significant sequence similarity to functionally characterized ADP/ATP carriers from other eukaryotes (17). In this paper, we analyzed these MCF proteins with regard to their predicted function as mitochondrial ATP/ADP carriers and assessed the importance of TbMCP5 for the energy metabolism of *T. brucei*.

## EXPERIMENTAL PROCEDURES

*Chemicals*—[$^3$H]ATR, N-ATR, and N-ADP were synthesized as described previously (18, 19). Succinate, α-ketoglutarate, ADP, ATP, ATR, bonkrekic acid (BA), carboxyatractyloside (CATR), and digitonin were purchased from Sigma-Aldrich. Luciferase and luciferin were from Roche Applied Science, and $Ap_5A$ and *n*-dodecyl-β-D-maltoside were from Calbiochem.

*Yeast Complementation*—The mitochondrial ADP/ATP carrier (ANC)-deficient *Saccharomyces cerevisiae* strain *JL1*Δ*2*Δ3 was cultured as described previously (20, 21). The complete open reading frames of *TbMCP5* (GeneDB Tb927.10.14820) and *TbMCP15* (GeneDB Tb927.8.1310) were PCR-amplified using the primer combination 5′-ggcgaattcatgacggataaaaagcggaaccgg-3′ (sense) and 5′-gcggatcccttaattcgatctgcgccactccacataaatgg-3′ (antisense) for *TbMCP5* and the primer combination 5′-ggcgaattcatggttggtggcgatggtgaggagc-3′ (sense) and 5′-gccggatcccttaggcagccggtaaaaaccacatatagagtgac-3′ (antisense) for *TbMCP15*. Restriction enzyme sites used for subsequent cloning into the yeast centromeric expression vector *pRS314* (see the *Saccharomyces* Genome Database) are underlined. Expression from *pRS314* takes place under the control of included *ScANC2* regulatory sequences (21). The resulting *TbMCP5-pRS314* and *TbMCP15-pRS314* constructs were used to transform *JL1*Δ*2*Δ*3u*$^-$ using a standard LiCl method. The rescue of non-fermentative growth of *JL1*Δ*2*Δ*3u*$^-$ by expression of ScAnc2p (positive control), TbMCP5, or TbMCP15 was assessed on solid YPL medium (glucose-free, lactate-containing rich medium) and compared with the fermentative growth on YNB Glc W$^-$ medium (tryptophan-free, glucose-supplemented minimal medium) (21).

*ADP/ATP Transport Assays for Yeast Mitochondria*—Yeast mitochondria were prepared by differential centrifugation (22). Briefly, yeast cells grown in YPL medium were harvested in the late log phase ($A_{600\,nm}$ ~5). Spheroplasts obtained after enzymatic digestion by Zymolyase 20T were disrupted by Dounce homogenization in 0.6 M mannitol, 10 mM Tris-HCl, pH 7.4, 1 mM EDTA, 0.1% (w/v) BSA, and 1 mM PMSF. Mitochondria were isolated by differential centrifugation, washed in the same buffer devoid of BSA and PMSF, and stored in liquid nitrogen. Mitochondrial ADP/ATP transport was measured using a luminescence assay as detailed by Dassa *et al.* (23). Briefly, freshly prepared mitochondria were incubated for 5 min at 25 °C in 10 mM Tris-HCl, pH 7.4, 10 mM $KH_2PO_4$, 0.6 M mannitol, 0.1 mM EGTA, 2 mM $MgCl_2$, 10 μM $Ap_5A$, and 1 mM α-ketoglutarate in the presence of 0.1% (w/v) luciferin and 0.1% (w/v) luciferase. ADP was added to initiate the mitochondrial ATP efflux. ATP production was determined by measuring the luciferase/luciferin-related light emission using a luminometer. Control experiments were carried out in the presence of the inhibitors CATR and BA, which specifically inhibit nucleotide exchange in ADP/ATP carriers.

*ATR and CATR Binding Assays*—[$^3$H]ATR binding assays with isolated yeast mitochondria were carried out as described previously (24). Mitochondria were diluted (1 mg of protein ml$^{-1}$) in 1 ml of MKE buffer (0.12 M KCl, 10 mM MOPS, pH 6.8, 1 mM EDTA), and [$^3$H]ATR was added at concentrations up to

6 μM. After incubation for 1 h at 4 °C, mitochondria were pelleted by centrifugation, and radioactivity associated with the pellet was determined using a liquid scintillation counter. Control experiments were performed in the presence of 20 μM CATR to correct for minor nonspecific [$^3$H]ATR binding. Fluorescence back-titration of CATR-binding sites was performed on mitochondria in MKE buffer in the presence of 1 μM N-ATR (25). The time course of the CATR-induced release of bound N-ADP was studied by incubating isolated mitochondria at 20 °C in MKE buffer (1 mg of protein ml$^{-1}$), and fluorescence was measured as described previously (26).

*Mitochondrial Cytochrome $aa_3$ Content*—The $aa_3$ cytochrome content of the isolated yeast mitochondrial fractions was determined by calculating the difference between recorded reduced and oxidized spectra at 550–650 nm (23). Briefly, mitochondria were diluted to 2 mg of protein ml$^{-1}$ in 100 mM $Na_2SO_4$, 10 mM Tris-HCl, pH 7.3, 1 mM EDTA, and 0.5% (w/v) *n*-dodecyl-β-D-maltoside. Cytochromes were oxidized or reduced by adding solid potassium ferricyanide or sodium dithionite, respectively. The extinction coefficient used for cytochrome $aa_3$ was 24,000 M$^{-1}$ cm$^{-1}$.

*TbMCP5 Peptide Antibody*—The peptide VDALKPIYVEWRRSN (amino acids 293–307 of TbMCP5) was coupled to KLH and used for the immunization of rabbits following a standard immunization protocol (EZBiolab). The αTbMCP5 antiserum was collected 9 weeks after first immunization and showed an antibody titer of 1:1,192,000. Western blot analysis (1:2,000 dilution) revealed a singly cross-reacting protein band with a molecular mass of 34 kDa, as predicted for TbMCP5 (17).

*Culture of T. brucei Cell Lines*—BSF and PCF *T. brucei* cell lines were cultured in HMI9 (27) and glucose-rich SDM79 medium (28), respectively. For growth experiments in the absence of glucose, PCF trypanosomes were cultured in glucose-depleted SDM80 medium (9). PCF *T. brucei* strains 449 and EATRO1125.T7T were used as "wild type" cell lines for all experiments and were cultured in the continuous presence of phleomycin (5 μg ml$^{-1}$) to maintain stable expression of the tetracycline repressor from plasmid pHD449 (29) or in the presence of G418 (10 μg ml$^{-1}$) and hygromycin (25 μg ml$^{-1}$) to maintain stable expression of the tetracycline repressor and T7 RNA polymerase from plasmids pLew90/Neo and pHD328, respectively (30). Trypanosomes were transfected as described previously (29, 31). The PCF cell line *TbMCP5-nmyc$^{ti}$* (17) was cultured in the presence of hygromycin (50 μg ml$^{-1}$); the conditional TbMCP5 double knock-out cell line Δ*TbMCP5/TbMCP5-nmyc$^{ti}$* was cultured in the presence of hygromycin (50 μg ml$^{-1}$), G418 (15 μg ml$^{-1}$), and blasticidin (10 μg ml$^{-1}$); and the EATRO1125.T7T RNAi mutant cell lines were cultured in the presence of hygromycin (25 μg ml$^{-1}$), G418 (10 μg ml$^{-1}$), and phleomycin (5 μg ml$^{-1}$). Cells were harvested at mid-logarithmic phase densities of $1 \times 10^6$ cells ml$^{-1}$ (BSF) and $1 \times 10^7$ cells ml$^{-1}$ (PCF) for protein and RNA analysis.

*Protein Quantification, Western Blot Analysis, and Immunofluorescence Microscopy*—Protein concentrations were determined using the bicinchoninic acid (BCA) reagent kit (Sigma-Aldrich) and BSA as the protein standard. The raised TbMCP5 antibody (this paper), an antibody against full-length ScAnc2p (21), and an antibody against heat shock protein 60 (HSP60) (32) were used for Western blot analysis at a dilution of 1:2,000, 1:1,500, and 1:10,000, respectively. Immunodetection was performed using horseradish peroxidase (HRP)-coupled protein A (Bio-Rad) or HRP-coupled Myc antibody (Santa Cruz Biotechnology, Inc., Santa Cruz, CA) and the enhanced chemiluminescence (ECL) kit from GE Healthcare. Immunofluorescence microscopy using paraformaldehyde-fixed trypanosomes was performed as described previously (17, 33). 4′,6-Diamidino-2-phenyl-indole (DAPI) was used for the specific staining of nuclear and kinetoplastid (mitochondrial) DNA, the mitochondrial marker MitoTracker (Invitrogen) was used for the specific labeling of *T. brucei* mitochondria (34), and the TbMCP5 antibody was used for the specific labeling of TbMCP5.

*Northern Blot Analysis*—Total RNA was isolated from trypanosomes using the RNeasy minikit (Qiagen). Northern blot analysis was performed as described by Sambrook *et al.* (35). The complete open reading frame of *TbMCP5* was labeled with [$^{32}$P]dCTP (PerkinElmer Life Sciences) using a standard PCR procedure. The RNA blot was prehybridized in hybridization buffer (5× SSC, 0.1% (w/v) SDS, 5× Denhardt's solution, 100 μg ml$^{-1}$ denatured and sheared salmon sperm DNA) for 30 min at 60 °C, after which the [$^{32}$P]dCTP-labeled DNA probe was added. After overnight hybridization at 60 °C, the blots were washed for 30 min in 1× SSC, 0.1% (w/v) SDS at room temperature, for 45 min in 1× SSC, 0.5% (w/v) SDS at 42 °C and for 30 min in 0.1× SSC, 0.2% (w/v) SDS at 42 °C, followed by autoradiographic detection.

*Generation of the Conditional TbMCP5 Double Knock-out Cell Line*—The previously generated PCF *T. brucei* cell line *TbMCP5-nmyc$^{ti}$* (17) allows the ectopic and tetracycline-inducible expression of recombinant N-terminal 2× Myc-tagged TbMCP5 and was used as the parental cell line for generation of the conditional TbMCP5 double knock-out cell line. The 5′-UTR of *TbMCP5a* (GeneDB Tb927.10.14820) and 3′-UTR of *TbMCP5c* (GeneDB Tb927.10.14840) were inserted on either side of the *NEO* (G418) or *BSD* (blasticidin) antibiotic resistance cassettes bearing actin 5′-splice sites and actin 3′-untranslated regions (36). The different UTRs were obtained by PCR from isolated *T. brucei* genomic DNA; the primer combination 5′-agggtgagctcgttctcagaagtgacttctgtcgcc-3′ (sense) and 5′-accgcactagtgtccatatgcaccagacgcggctagtcg-3′ (antisense) was used for the 678-bp 5′-UTR of *TbMCP5a*, whereas the primer combination 5′-ctcaccaggatccgtgccgttgctggtttttattg-3′ (sense) and 5′-ccttgggcccctcctcaggcacagccttaccgtttt-3′ (antisense) was used for the 724-bp 3′-UTR of *TbMCP5c*. The underlined restriction enzyme sites were used for subsequent cloning in the different *NEO*- and *BSD*-containing knock-out (KO) plasmids. After transfection of *TbMCP5-nmyc$^{ti}$* with the *NEO-TbMCP5*-KO construct and clonal selection with 15 μg ml$^{-1}$ G418, the half-knock-out cell line Δ*TbMCP5*::*NEO/TbMCP5/TbMCP5-nmyc$^{ti}$* was isolated. The double knock-out cell line Δ*TbMCP5*::*NEO*/Δ*TbMCP5*::*BSD/TbMCP5-nmyc$^{ti}$*, further referred to as Δ*TbMCP5/TbMCP5-nmyc$^{ti}$* in this paper, was obtained after subsequent transfection with the *BSD-TbMCP5*-KO plasmid, followed by clonal selection with 15 μg ml$^{-1}$ G418 and 10 μg ml$^{-1}$ blasticidin. The *TbMCP5a* to *-c* half- and double knock-out cell lines were cultured in the continuous presence of tetracycline (1 μg ml$^{-1}$) in order to main-

tain TbMCP5-nmyc expression and cell viability. Correct integration of the different *NEO/BSD-TbMCP5*-KO constructs and deletion of the two native *TbMCP5a* to *-c* gene clusters was confirmed by Southern blot analysis and PCR (results not shown) as well as by Western blot analysis for the TbMCP5 gene product (this paper).

*ATP Production by T. brucei Mitochondria*—Mitochondrial ATP production in *T. brucei* was analyzed according to Schneider *et al.* (13). Briefly, $1 \times 10^8$ trypanosomes were harvested and permeabilized with 0.008% (w/v) digitonin. A mitochondria-enriched subcellular fraction was obtained after centrifugation and extensive washing in SoTE buffer (20 mM Tris-HCl, pH 7.5, 2 mM EDTA, 0.6 M Sorbitol). The mitochondria-enriched subcellular fraction was resuspended in ATP Assay Buffer (20 mM Tris-HCl, pH 7.4, 15 mM $KH_2PO_4$, 5 mM $MgSO_4$, 0.6 M Sorbitol), and mitochondrial ATP production was initiated by the addition of 67 $\mu$M ADP and 5 mM succinate or 5 mM $\alpha$-ketoglutarate (13). The specific ADP/ATP carrier inhibitor CATR (4 $\mu$g ml$^{-1}$) was added during control experiments. ATP formation was quantified using the ATP Bioluminescence Assay Kit CLS II (Roche Applied Science) in combination with a luminometer.

*Metabolite Analysis*—Wild type and TbMCP5-depleted Δ*TbMCP5/TbMCP5-nmyc*$^{ti}$ trypanosomes were cultured for 72 h in glucose-depleted SDM80 medium. Culture aliquots were collected every 24 h for the determination of cell density (cells ml$^{-1}$). Proline consumption was determined as described previously (37), whereas product formation, here succinate and acetate, was determined using corresponding detection kits from Megazyme.

*Depletion of TbMCP5 by RNA Interference*—Inhibition of *TbMCP5* gene expression was performed in PCF *T. brucei* by using RNA interference (RNAi) (38). The 563-bp sense and 624-bp antisense sequences of *TbMCP5* were PCR-amplified and cloned into the *T. brucei* expression vector *pLew100* (39). The primer combination 5′-gtgtataagctttggcgaggtaacctgtca-3′ and 5′-gtcatcctcgagcgccggcgaacggtgtccaa-3′ was used for amplification of the 563-bp sense *TbMCP5* sequence, and the primer combination 5′-gggcgtggatccgctttggcgaggtaacctgtc-3′ and 5′-tgcaacaagctttccctcgagttcttgtacttcacagcagc-3′ was used for the 624-bp antisense *TbMCP5* sequence. The underlined restriction enzyme sites were used for cloning into *pLew100*. The resulting *pLew100-TbMCP5* RNAi construct harbors a phleomycin resistance gene and contains the consecutively cloned sense and antisense *TbMCP5* target sequences separated by a 50-bp spacer fragment. Inducible expression is under control of the procyclic acidic repetitive protein promoter linked to a prokaryotic tetracycline operator (39). The *pLew100-TbMCP5* RNAi construct was used for transfection of procyclic form *T. brucei* EATRO1125-T7T (30). The mutant $^{RNAi}$*TbMCP5* cell line was obtained after clonal selection in glucose-rich SDM79 medium containing hygromycin (25 $\mu$g ml$^{-1}$), neomycin (10 $\mu$g ml$^{-1}$), and phleomycin (5 $\mu$g ml$^{-1}$). This cell line enables inducible depletion of TbMCP5 on a wild type PCF background. The *pLew100-TbMCP5* RNAi construct was further used for transfection of the previously generated PCF *T. brucei* knock-out mutant Δ*pepck*-cl1, which lacks the gene coding for phosphoenolpyruvate carboxykinase (PEPCK) (10). The mutant cell line Δ*pepck*/$^{RNAi}$*TbMCP5* was obtained after clonal selection in glucose-rich SDM79 medium containing puromycin (1 $\mu$g ml$^{-1}$), hygromycin (25 $\mu$g ml$^{-1}$), neomycin (10 $\mu$g ml$^{-1}$), and phleomycin (5 $\mu$g ml$^{-1}$). This cell line enables inducible depletion of TbMCP5 on a *pepck* null background. The obtained mutant cell lines were subsequently adapted to glucose-depleted SDM80 medium, containing the same antibiotics. The addition of tetracycline to the PCF $^{RNAi}$*TbMCP5* and Δ*pepck*/$^{RNAi}$*TbMCP5* cell lines will lead to the expression of double-stranded *TbMCP5* RNA molecules and the concomitant down-regulation (silencing) of TbMCP5 expression.

## RESULTS

*Sequence Analysis of TbMCP5 and TbMCP15*—TbMCP5 and TbMCP15 have previously been identified as novel members of the *T. brucei* mitochondrial carrier family (17). The *T. brucei* genome contains three identical and consecutive arranged genes coding for TbMCP5 (*i.e. TbMCP5a* to *-c* (GeneDB Tb927.10.14820/830/840), whereas TbMCP15 is coded for by a single gene (GeneDB Tb927.8.1310) (17). TbMCP5 and TbMCP15 contain sequence features that are conserved in all MCF proteins (14), including the presence of six trans-membrane helices, a tripartite protein domain structure with semiconserved sequence repeats of ~100 amino acids, and the canonical signature sequence motif, P*X*(D/E)$X_2$(K/R)*X*(K/R)$X_{20-30}$(D/E)G$X_{4-5}$(W/F/Y)(K/R)G, at the end of each odd-numbered trans-membrane helix (Fig. 1*A*). They are further the only two members of the *T. brucei* MCF inventory that share significant sequence similarity (67–84% amino acid identity (17)) with functionally characterized ADP/ATP carriers from other eukaryotes, such as *S. cerevisiae* Anc2p (24) and *Homo sapiens* Anc1p (20).

The hallmark of ADP/ATP carriers is the presence of the conserved hexapeptide sequence RRRMMM (40). Mutation analysis confirmed that this motif is involved in ADP binding and is essential for ADP/ATP exchange (41). Also TbMCP5 contains a conserved RRRMMM motif (Fig. 1*B*), supporting the prediction that this MCF protein functions as an ADP/ATP carrier. MCF proteins further contain several conserved amino acids that are involved in the selective binding and transport of substrates. These amino acids are organized in three distinct substrate contact points (CP1 to -3; Fig. 1*B*) and are conserved for MCF proteins that transport similar substrates (42). For ADP/ATP carriers, CP1 is composed of the three conserved amino acids arginine, threonine, and asparagine, corresponding to Arg-96, Thr-100, and Asn-104, respectively, of the ScAnc2p reference sequence; CP2 is composed of a conserved glycine and isoleucine, here Gly-199 and Ile-200 in ScAnc2p; and CP3 is composed of only a single amino acid and is, in the case of ADP/ATP carriers, represented by a conserved arginine, Arg-294, in ScAnc2p (Fig. 1*B*). Sequence comparison revealed that in TbMCP5 the amino acid compositions of the three different substrate contact points were identical to those of ScAnc2p and HsAnc1p (Fig. 1*B*). In addition, TbMCP5 contains a well conserved aromatic ladder, corresponding to Tyr-203, Tyr-207, Phe-208, and Tyr-211 in the ScAnc2p reference sequence (Fig. 1*B*), which is crucial for ADP/ATP exchange in ADP/ATP carriers (26). All of these observations reinforced the predicted ADP/ATP carrier function of TbMCP5.

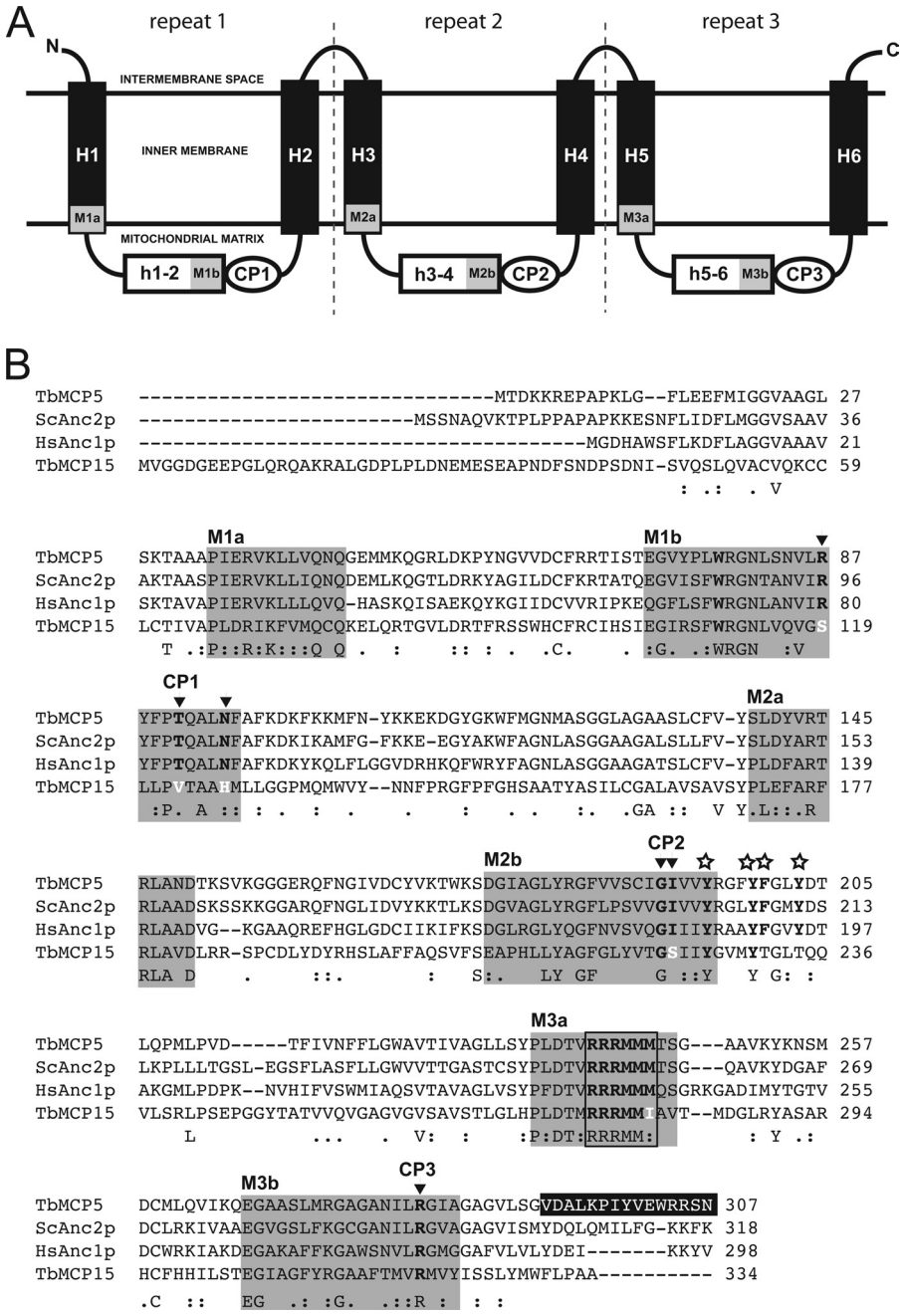


FIGURE 1. **TbMCP5 contains conserved ADP/ATP carrier sequence features.** *A*, schematic representation of MCF protein sequence structure. Trans-membrane helices are represented by *H1–H6*, whereas the connecting hydrophilic loops are represented by *h1–2*, *h3–4*, and *h5–6*, respectively. *M1–M3a* indicate the first part (P*X*(D/E)*XX*(K/R)*X*(K/R)), and *M1–M3b* indicate the second part ((D/E)G$X_n$(K/R)G) of the canonical MCF signature sequence. The different conserved substrate contact points are indicated by *CP1–CP3*. *B*, sequence alignment of TbMCP5 and TbMCP15 with *S. cerevisiae* Anc2p (*ScAnc2p*) and *H. sapiens* Anc1p (*HsAnc1p*). The different parts of the canonical signature sequence (see *A*) are indicated by *gray backgrounds*. *Open stars* indicate conserved amino acids of the aromatic ladder. Conserved amino acids of the different substrate contact points (*CP1–CP3*) are printed in *black boldface type* and indicated by *arrows*, whereas deviating amino acids are printed in *white boldface type*. The conserved hexapeptide sequence RRRMMM found in all ADP/ATP carriers is *boxed*. The C-terminal peptide sequence of TbMCP5 used for immunization is shown in *white* on a *black background*.

In contrast, TbMCP15 contains a degenerated version of the RRRMMM motif, with a single amino acid substitution (Met to Ile) at position 3 of the methionine cluster (Fig. 1*B*). A similar mutation of the methionine cluster in ScAnc2p resulted in the elimination of ADP/ATP exchange activity (41). In addition, the amino acid compositions of CP1 to -3 are different from those of conventional ADP/ATP carriers; in particular, CP1 is not conserved at all (Fig. 1*B*). TbMCP15 further contains a degenerated aromatic ladder (Fig. 1*B*). Overall, these deviations strongly suggest that TbMCP15 is not a classical ADP/ATP exchanger, despite its overall sequence similarity to ADP/ATP carriers from other eukaryotes.

*Functional Complementation Analysis of S. cerevisiae JL1Δ2Δ3u⁻*—The *S. cerevisiae* deletion strain *JL1Δ2Δ3u⁻* is deficient in mitochondrial ADP/ATP carriers (*ANC*-deficient) and is only viable on a fermentable carbon source, such as glucose (21). The putative ADP/ATP exchange function of *TbMCP5* and *TbMCP15* can therefore be directly assessed *in*

*vivo* by testing their ability to restore growth of *JL1*Δ*2*Δ*3u*$^-$ cells on glucose-depleted YPL medium, containing lactate as a non-fermentable carbon source (21, 43). The open reading frames of *TbMCP5* and *TbMCP15* were cloned into the low copy number yeast expression vector *pRS314*, containing *ScANC2* regulatory regions (21). *pRS314*, containing the *ScANC2* ORF, was used as a positive control, whereas *pRS314* without any insert was used as a negative control. The *JL1*Δ*2*Δ*3u*$^-$ strain was transformed with the various constructs to produce the *JL-TbMCP5*, *JL-TbMCP15*, and *JL-ScANC2* strains. Growth of these strains was examined on solid YPL medium and glucose-rich tryptophan-free YNB medium (YNB Glc W$^-$). As expected, growth of all strains was similar when plated on YNB Glc W$^-$ medium, whereas growth of *JL1*Δ*2*Δ*3u*$^-$ on YPL medium was restored to wild-type level with the expression of ScAnc2p (*JL-ScANC2*) but not with the empty *pRS314* vector (Fig. 2*A*). TbMCP15 could not restore growth of *JL1*Δ*2*Δ*3u*$^-$ (*JL-TbMCP15*) on YPL medium, which confirmed the *in silico* prediction that TbMCP15 is not an ADP/ATP carrier (Fig. 2*A*). Expression of TbMCP5 in *JL1*Δ*2*Δ*3u*$^-$ yeast cells (*JL-TbMCP5*) resulted in a significant rescue of growth on YPL medium (Fig. 2*A*). This result confirmed that TbMCP5 is able to functionally complement the mitochondrial ADP/ATP carrier deficiency of yeast. However, the functional complementation is not optimal; for *JL-TbMCP5*, a doubling time of 6 h was found at the plateau phase of its growth, whereas for *JL-ScANC2*, the doubling time was significantly shorter, here 2.5 h at the same growth phase (Table 1).

*Mitochondrial Localization and Quantification of TbMCP5 in JL1*Δ*2*Δ*3u*$^-$—Growth of *JL-TbMCP5* on YPL medium was completely inhibited by the addition of the specific ADP/ATP carrier inhibitors CATR and BA (not shown). These results not only confirmed that TbMCP5 functions as an ADP/ATP carrier but also implied that TbMCP5 has the expected mitochondrial localization in *JL-TbMCP5*. The mitochondrial location of TbMCP5 was further investigated by subcellular fractionation and Western blot analysis, using a polyclonal antibody directed against ScAnc2p (21) and the TbMCP5 antibody described in this paper (see below). Mitochondria were isolated by differential centrifugation from the *JL-TbMCP5* and *JL-ScANC2* strains (22). As expected, the ScAnc2p antibody readily detected the Anc2p protein in the mitochondrial fraction of *JL-ScANC2* (Fig. 2*B*, *left*, *lane 1*). In addition, a smaller cross-reacting protein band was observed (Fig. 2*B*, *left*, *lane 1*), which most probably represents a ScAnc2p degradation product resulting from the mitochondrial preparation. The ScAnc2p antibody was further able to stain the heterologous TbMCP5 protein in the *JL-TbMCP5* mitochondria, although the observed signal was rather faint (Fig. 2*B*, *left*, *lane 2*). Staining with the TbMCP5 antibody resulted in a single strong signal of the expected size and confirmed the presence of TbMCP5 in the mitochondrial fraction of *JL-TbMCP5* (Fig. 2*B*, *right*, *lane 2*). These results unambiguously correlated the restoration of *JL1*Δ*2*Δ*3u*$^-$ growth on YPL medium with the presence of TbMCP5 protein in the yeast mitochondria.

The amount of TbMCP5 present in *JL-TbMCP5* mitochondria was estimated by determining the number of ATR-binding sites via titration using specific ADP/ATP carrier inhibitors (25). Interaction parameters were measured directly using the specific high affinity labeled radioactive ligand [$^3$H]ATR or indirectly via a fluorescence back-titration assay with N-ATR, assuming that 1 mol of ATR binds to 1 mol of analyzed ADP/ATP carrier (25). As expected, the binding of [$^3$H]ATR to *JL-TbMCP5* mitochondria increased as a function of the concentration of [$^3$H]ATR added and finally reached saturation (Fig. 2*C*). The binding isotherm was deduced from the Scatchard plot (Fig. 2*C*, *inset*). The maximum number of ATR-binding sites ($B_{max}^{ATR}$) and the ATR dissociation constant ($K_D^{ATR}$) were determined for TbMCP5 and compared with those obtained for ScAnc2p (Table 1). The $K_D^{ATR}$ measured for ScAnc2p and TbMCP5 were in the same range, here 396 ± 23 and 503 ± 15 nM, respectively (Table 1), indicating that both carriers have similar ATR-binding properties. However, the $B_{max}^{ATR}$ of TbMCP5 (149 ± 17 pmol mg$^{-1}$ protein) is about 5 times lower than the $B_{max}^{ATR}$ of ScAnc2p (698 ± 51 pmol mg$^{-1}$ protein) (Table 1). To exclude the possibility that the observed difference in $B_{max}^{ATR}$ is due to differences in protein concentration, cytochrome $aa_3$ was quantified for the different mitochondrial fractions. Analysis revealed that the cytochrome $aa_3$ concentrations were similar for the different mitochondrial fractions (*i.e.* 200 ± 23 *versus* 188 ± 32 pmol mg$^{-1}$ of cytochrome $aa_3$, respectively) (Table 1). Binding of ATR to isolated mitochondria was estimated by measuring fluorescence variation of bound N-ATR in competition with added CATR (Fig. 2*D*). The maximum amount of CATR-binding sites was estimated to be 160 pmol mg$^{-1}$, which is in agreement with the obtained [$^3$H]ATR titration data (149 pmol mg$^{-1}$ protein). These results indicated that TbMCP5 was about 4-fold less abundant than ScAnc2p in the isolated mitochondrial fractions, which in turn could account for the reduced growth of *JL-TbMCP5* on YPL medium.

*ADP/ATP Transport Kinetics of TbMCP5 in Comparison with ScAnc2p*—The ADP/ATP exchange activity of TbMCP5 in *JL-TbMCP5* mitochondria was determined as described previously (23). Mitochondria isolated from ScAnc2p-expressing yeast cells (*JL-ScANC2*) were used for comparison. As expected, no ADP/ATP exchange was found for both mitochondrial preparations in the presence of the specific ADP/ATP carrier inhibitors CATR and BA (not shown). The obtained Michaelis-Menten and Lineweaver-Burk plots (Fig. 2*E*) were used to determine the variation in exchange rate as a function of ADP concentration for TbMCP5 and ScAnc2p (Table 1). Comparison of the obtained kinetic parameters revealed that the $V_{max}$ of TbMCP5 was about 4.5 times lower than the $V_{max}$ of ScAnc2p (Table 1). This result is in agreement with the lower amount of TbMCP5 present in yeast mitochondria compared with ScAnc2p. Comparison revealed further that the $k_{cat}$ values and $K_m$ values of external free ADP were similar for TbMCP5 and ScAnc2p (Table 1). The fluorescent compound N-ADP is a non-transportable ADP analog. Its fluorescence is quenched upon binding to ADP/ATP carriers, so specific binding to the mitochondrial ScAnc2p or TbMCP5 can be measured by the enhancement of fluorescence upon dissociation after the addition of CATR (Fig. 2*F*). ADP-binding experiments revealed that the $K_{½}$ value of N-ADP binding to TbMCP5 is 6.2 μM, which is similar to the value found for ScAnc2p, here 5.1 μM (Table 1).

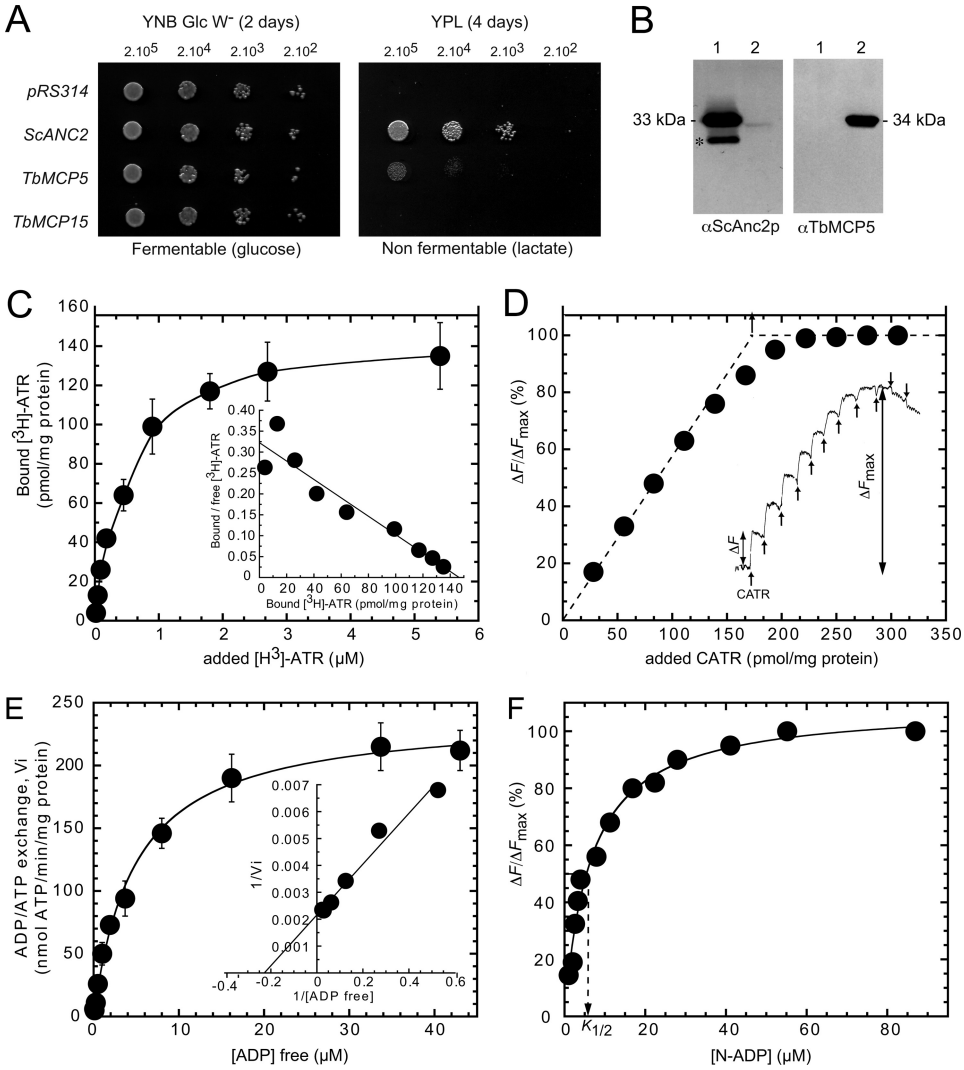


FIGURE 2. **TbMCP5 functions as a mitochondrial ADP/ATP carrier.** *A*, yeast growth phenotype associated with the expression of TbMCP5 and TbMCP15. The *ANC*-deficient *S. cerevisiae* strain *JL1Δ2Δ3u*$^-$ was transformed with *pRS314* (no insert) and *pRS314* containing *ScANC2*, *TbMCP5*, or *TbMCP15*. Yeast cell lines were isolated and inoculated in liquid minimum tryptophan-free medium containing 2% (v/v) glucose as a carbon source (YNB Glc W$^-$). Log phase cultures were diluted to $2 \times 10^3$ to $2 \times 10^5$ cells/5 ml before spotting onto YNB Glc W$^-$ or lactate-containing medium (YPL) plates and incubated at 28 °C for 2 days (YNB) or 4 days (YPL). *B*, immunodetection of TbMCP5 and ScAnc2p in yeast mitochondria. Mitochondrial extracts (20 mg of protein/lane) prepared from *JL-ScANC2* (*lanes 1*) and *JL-TbMCP5* (*lanes 2*) strains were subjected to SDS-PAGE (12.5% (w/v) acrylamide) and Western blot analysis using a polyclonal rabbit antibody (αScAnc2p) directed against the complete ScAnc2p sequence and the TbMCP5 peptide antibody (αTbMCP5; this paper). *C*, specific binding of [$^3$H]ATR to mitochondria expressing TbMCP5. Isolated mitochondria (1 mg of total protein) from yeast cells expressing TbMCP5 were incubated with increasing concentrations of [$^3$H]ATR. After centrifugation, the radioactivity associated with the mitochondrial pellet was estimated by scintillation counting. Data were corrected for nonspecific binding from parallel experiments carried out in the presence of 20 μM CATR. The *inset* shows the Scatchard plot of the binding data. *Error bars* were calculated from three independent experiments. *D*, fluorescence back-titration of CATR-binding sites to quantify the amount of TbMCP5 in mitochondria. Mitochondria (0.9 mg of protein ml$^{-1}$) were suspended at 20 °C in 2 ml of MKE buffer containing 1 μM of N-ATR. Fluorescence variations (Δ*F*) induced by additions of CATR (25 pmol for each addition) were recorded as a function of time and are shown as an *inset*. $\Delta F/\Delta F_{max}$ was plotted as a function of added CATR per mg of total proteins. *E*, ADP/ATP transport activity of TbMCP5 in isolated mitochondria. ADP/ATP transport was measured by means of a luciferase-based ATP assay. Freshly prepared mitochondria were energized in the presence of 5 μM of α-ketoglutarate (as respiratory substrate), the adenylate kinase inhibitor $Ap_5A$, and of 0.1% (w/v) luciferin and 0.1% (w/v) luciferase. After a 3-min incubation period, free ADP (0.06–43 μM final concentration calculated using WinMaxc version 2.05 software) was added to initiate the ATP efflux, and the related light emission was recorded. The time course of ATP efflux was monitored over a 5-min period. Control experiments were carried out in the presence of 20 μM CATR to ensure that the ADP/ATP exchange was mediated by ADP/ATP carriers. Quantification of released ATP was performed on the basis of the signal amplitude corresponding to additions of 0.5 nmol of ATP as a standard. Kinetic data were plotted using the graphical representations of Michaelis-Menten and Lineweaver-Burk (*inset*). The shown values are the means of three independent experiments. *F*, fluorescence titration of N-ADP-binding sites. The time course of CATR-induced release of bound N-ADP was studied by incubating isolated mitochondria (1 mg of mitochondrial proteins ml$^{-1}$) in the presence of N-ADP (0.5–87 μM). Thereafter, the fluorescence level was set to zero. The increase in fluorescence induced upon the addition of 5 μl of 2 mM CATR (Δ*F*) was recorded until it became stable. The apparent dissociation constant $K_{1/2}$ was determined after plotting $\Delta F/\Delta F_{max}$ as a function of added N-ADP concentration. *Error bars*, S.D.

This similarity in ADP-binding is further in agreement with the observed small difference in $K_m$ value for external free ADP (Table 1). Overall, ScAnc2p and TbMCP5 present comparable biochemical properties with regard to their ADP/ATP exchange activity in yeast mitochondria.

*TbMCP5 Is Exclusively Mitochondrial and Differentially Expressed in T. brucei*—We previously reported that TbMCP5 has an exclusive mitochondrial localization in the procyclic life cycle stage of *T. brucei* (17). This subcellular localization was determined by immunofluorescence microscopy using a

**TABLE 1**

**Yeast growth properties, ligand-binding data for carriers, and kinetic parameters of ADP/ATP transport activity measured in mitochondria isolated from *JL-ScANC2* and *JL-TbMCP5***

All of the values are the means of three independent experiments.

| Yeast strains | *JL-ScANC2* | *JL-TbMCP5* |
|---|---|---|
| **Cell culture in YPL**[a] | | |
| Doubling time (h) | 2.5 | 6 |
| Growth yield $A_{600\ nm}$ | 12 | 11 |
| **[$^3$H]ATR binding**[b] | | |
| $B_{max}$ (pmol mg protein$^{-1}$) | 698 ± 51 | 149 ± 17 |
| $K_d$ (nM) | 396 ± 23 | 503 ± 15 |
| Cytochrome $aa_3$ (pmol mg$^{-1}$)[c] | 200 ± 23 | 188 ± 32 |
| **ADP/ATP exchange**[d] | | |
| $V_{max}$ (nmol ATP min$^{-1}$ mg protein$^{-1}$) | 1,046 ± 173 | 240 ± 17 |
| $k_{cat}$ (min$^{-1}$) | 1,424 ± 101 | 1,619 ± 85 |
| $K_m$ external ADP ($\mu$M) | 4.6 ± 0.8 | 4.2 ± 0.1 |
| **N-ADP dissociation constant**[e] | | |
| $K_{½}$ | 6.2 ± 0.7 | 5.1 ± 0.5 |

[a] Cells were cultivated on liquid YPL medium.
[b] [$^3$H]ATR binding parameters. The number of binding sites, $B_{max}$ and $K_d$ values were calculated from Scatchard plots of [$^3$H]ATR binding data.
[c] The cytochrome $aa_3$ content of isolated mitochondria was measured by recording the reduced minus oxidized visible spectrum. $\epsilon_{aa3} = 24{,}000\ M^{-1}\ cm^{-1}$.
[d] $V_{max}$ and apparent $K_m$ for external free ADP were calculated from kinetic data using the Michaelis-Menten and Lineweaver-Burk equations. $k_{cat}$ refers to carrier turnover, calculated based on the carrier content determined by [$^3$H]ATR-binding experiments, assuming that 1 mol of ATR binds to 1 mol of transport unit.
[e] The $K_{½}$ value was determined by plotting $\Delta F/\Delta F_{max}$ as a function of added N-ADP.

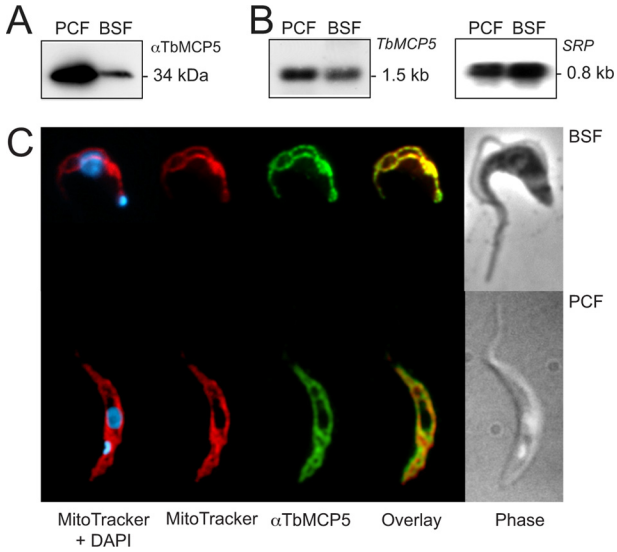


FIGURE 3. **TbMCP5 is exclusively mitochondrial and differentially expressed.** *A*, Western blotting analysis of wild type PCF and BSF *T. brucei* using the αTbMCP5 antibody (diluted 1:2,000). Each lane contained $2 \times 10^6$ trypanosomes. *B*, Northern blot analysis of total RNA from PCF and BSF *T. brucei* using [α-$^{32}$P]dCTP-labeled *TbMCP5* DNA as a probe for hybridization. Each lane contained 20 μg of total RNA. *C*, immunofluorescence microscopy of wild type BSF and PCF *T. brucei*, confirming the exclusive mitochondrial localization of TbMCP5. TbMCP5 was stained (*green*) using the αTbMCP5 antibody (diluted 1:500). Mitochondria were stained (*red*) with the specific mitochondrial marker Mitotracker, whereas nuclear and kinetoplast DNA was stained (*blue*) with DAPI.

*T. brucei* cell line expressing recombinant N-terminal Myc-tagged TbMCP5 (*TbMCP5-nmyc$^{ti}$*) and a commercial Myc antibody (17). To assess the expression and subcellular localization of the native protein, a polyclonal rabbit antiserum was raised against the C-terminal peptide 293–307 of TbMCP5. Western blot analysis using the TbMCP5 peptide antibody revealed a single cross-reacting protein band with the expected molecular size of 34 kDa in both the PCF and BSF of *T. brucei* strain 449 (Fig. 3*A*). Quantification of the obtained Western blot signals revealed that about 4.5-fold more TbMCP5 is present in PCF *T. brucei* compared with the BSF parasite. This differential expression of TbMCP5 is supported by Northern blot analysis, which revealed about 2.5-fold more *TbMCP5* mRNA in PCF *T. brucei* (Fig. 3*B*). Immunofluorescence microscopy showed specific tubular staining patterns for both PCF and BSF *T. brucei* when using the TbMCP5 peptide antibody (Fig. 3*C*). These staining patterns were identical to those obtained for the mitochondrial marker MitoTracker (Fig. 3*C*) (34). These results confirmed the expression and mitochondrial localization of TbMCP5 in the two different life cycle stages of *T. brucei* and indicated further that TbMCP5 is more abundant in PCF *T. brucei*.

*Silencing and Depletion of TbMCP5 in PCF Trypanosomes*—Different approaches were used to silence TbMCP5 expression in PCF *T. brucei*. Initially, a conventional targeted gene replacement method was used to replace the two chromosomal *TbMCP5a* to *-c* gene clusters (diploid organism) through consecutive homologous recombination using different antibiotic-resistant cassettes. The upstream *TbMCP5a* 5′-UTR and downstream *TbMCP5c* 3′-UTR were used for homologous recombination, allowing each *TbMCP5a* to *-c* gene cluster to be removed in a single recombination event. However, using this conventional method, no viable *TbMCP5a* to *-c* double knock-out clones could be obtained on glucose-rich SDM79 or glucose-depleted SDM80 medium, suggesting that expression of TbMCP5 is essential for growth. To overcome the apparent lethal phenotype, a recombinant tetracycline-inducible and nmyc-tagged version of *TbMCP5* (inducible rescue copy) was inserted into the *T. brucei* genome prior to the deletion of the two endogenous *TbMCP5a* to *-c* gene clusters. The addition of tetracycline to the obtained *TbMCP5-nmyc$^{ti}$* cell line resulted in the expression of recombinant Myc-tagged TbMCP5 (TbMCP5-nmyc; 37 kDa), whereas tetracycline withdrawal resulted in the absence (below the detection limit of the method used) of the same protein (Fig. 4*A*). The tetracycline-induced *TbMCP5-nmyc$^{ti}$* cell line was subsequently used to generate the conditional TbMCP5 double knock-out cell line Δ*TbMCP5/TbMCP5-nmyc$^{ti}$*. Western blot analysis (Fig. 4*B*) of the tetracycline-induced Δ*TbMCP5/TbMCP5-nmyc$^{ti}$* cell line confirmed the absence of endogenous TbMCP5a to -c (34 kDa) and the presence of recombinant TbMCP5-nmyc (37 kDa). Subsequent withdrawal of tetracycline resulted in the depletion (below detection limit) of *TbMCP5-nmyc* mRNA within 24 h (Fig. 4*C*). As expected, also the corresponding TbMCP5-nmyc protein level decreased significantly, although some recombinant protein could still be detected at 72 h (Fig. 4*C*). Withdrawal of tetracycline for more than 72 h resulted in loss of expression control and an increased expression of TbMCP5-nmyc (not shown). This loss of expression control upon gene deletion or silencing is common for *T. brucei*, especially if the target gene is essential for growth/survival of the parasite (31).

Analysis of the non-induced Δ*TbMCP5/TbMCP5-nmyc$^{ti}$* cell line revealed a partial growth defect in glucose-depleted medium (SDM80) compared with growth of the wild type cell

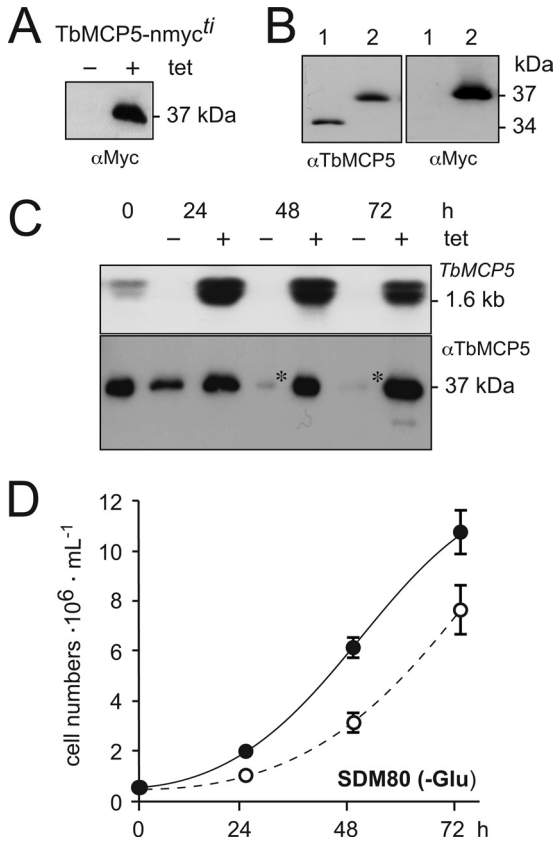


FIGURE 4. **Analysis of the conditional Δ*TbMCP5/MCP5-nmyc^ti* cell line.** *A*, Western blot analysis of *TbMCP5-nmyc^ti* cells grown without (−) or in the presence (+) of tetracycline. Each lane contained $2 \times 10^6$ trypanosomes. TbMCP5-nmyc protein was stained with a Myc antibody (αMyc). *B*, Western blot analysis of protein extracts from wild type (*lanes 1*) and tetracycline-induced Δ*TbMCP5/TbMCP5-nmyc^ti* (TbMCP5-nmyc-expressing; *lanes 2*) trypanosomes, using the TbMCP5 antibody (αTbMCP5) and αMyc. Each lane contained $2 \times 10^6$ trypanosomes. *C*, the conditional Δ*TbMCP5/MCP5-nmyc^ti* cell line was cultured in SDM80 medium with (+, induced) or without (−, non-induced) tetracycline. Samples were taken every 24 h for Northern blot analysis (*top*) using the [α-$^{32}$P]dCTP-labeled *TbMCP5* ORF DNA as hybridization probe and for Western blot analysis using αTbMCP5. Each *lane* contained 20 μg of total RNA (*top*; Northern blot analysis) or $2 \times 10^6$ trypanosomes (*bottom*; Western blot analysis). *Asterisks* indicate residual TbMCP5-nmyc protein. *D*, cumulative growth curve of wild type (*solid line*) and non-induced Δ*TbMCP5/MCP5-nmyc^ti* trypanosomes (TbMCP5-depleted; *dashed line*) grown in glucose-depleted SDM80 medium. Cell densities (cells ml$^{-1}$) were determined every 24 h, and means are derived from six independent experiments. *Error bars*, S.D.

line in the same medium (Fig. 4*D*). This result was somewhat unexpected because TbMCP5 was proposed to be essential for trypanosome growth; thus, its deletion should lead to a severe and probably lethal growth defect. However, the residual TbMCP5-nmyc protein observed for the non-induced Δ*TbMCP5/TbMCP5-nmyc^ti* cell line (Fig. 4*C*) is apparently sufficient to support substantial growth of the parasite.

Alternatively to the above described conventional and conditional gene replacement methods, we down-regulated the expression of TbMCP5 in wild type *T. brucei* through RNAi. Western blot analysis of the obtained *RNAi TbMCP5* cell line showed that when cultured on glucose-rich SDM79 or glucose-depleted SDM80 medium, TbMCP5 was completely depleted (below the detection limit of the method used) within 48 h after induction of the RNAi (Fig. 5*C*). TbMCP5 remained depleted for up to 7 days, after which it slowly reappeared (Fig. 5*C*). In glucose-rich SDM79 medium, growth of the *RNAi TbMCP5* cell line was reduced until day 7 after induction (*arrow* in Fig. 5*A*). However, with the reappearance of TbMCP5 after day 7 (Fig. 5*C*), it reverted to wild type growth, suggesting that TbMCP5 is essential for growth under glucose-rich conditions. Interestingly, the same cell line was unable to grow in glucose-depleted SDM80 medium (Fig. 5*B*), although TbMCP5 was re-expressed after day 7 (Fig. 5*C*). This result suggested that TbMCP5 plays a more important role when glucose is absent from the medium. In the absence of glucose, ATP can only be generated via mitochondrial oxidative phosphorylation from proline degradation (9–11). This process is in turn dependent on the presence of a functional ADP/ATP carrier in the inner mitochondrial membrane, which replenishes ADP in the mitochondrion and provides essential ATP to the rest of the cell. The inability of TbMCP5-depleted PCF *T. brucei* to grow on glucose-depleted SDM80 medium was therefore expected. In the presence of glucose, however, ATP can be produced in the cytosol during the final two steps (phosphoglycerate kinase and pyruvate kinase) of the cytosolic part of the glycolytic pathway. PCF *T. brucei* is therefore not exclusively dependent on the mitochondrion for its cellular ATP provision (9, 11).

To confirm this hypothesis, we subsequently down-regulated TbMCP5 expression on a PEPCK null background. PEPCK is the first enzyme in the glycosomal succinic fermentation branch and is required for sustaining the ADP/ATP and redox balances in the glycosome (10). Deletion of the PEPCK-coding gene in PCF *T. brucei* was previously shown to ablate the glycosomal production of succinate (10). The resulting Δ*pepck* cell line is primarily dependent on the mitochondrial degradation of proline as consequence of a substantial decrease in glucose consumption, even under glucose-rich conditions (10). RNAi-mediated depletion of TbMCP5 on a *PEPCK* null background (Δ*pepck*/*RNAi TbMCP5*) resulted in cell death 7 days after induction in both glucose-rich and glucose-depleted media (Fig. 5, *D* and *E*). The absence of TbMCP5 in both experiments was confirmed by Western blot analysis (Fig. 5*F*). The rapid death of the TbMCP5-depleted Δ*pepck*/*RNAi TbMCP5* cell line under both growth conditions reflects its now proline-dependent metabolism, irrespective of the glucose concentrations in the different culture media (*i.e.* 6 mM in SDM79 *versus* <0.15 mM in SDM80). Remarkably, the Δ*pepck* cell line is more sensitive to RNAi-mediated depletion of TbMCP5 than wild type cells, even under glucose-depleted conditions. This may be due to the presence of the residual <0.15 mM glucose in SDM80, which could be used for growth by the *RNAi TbMCP5* single mutant but not by the Δ*pepck*/*RNAi TbMCP5* double mutant. Altogether, these data showed that TbMCP5 is essential for PCF *T. brucei*, particularly in a glucose-depleted environment where ATP is primarily produced in the mitochondrion from proline metabolism.

*TbMCP5 Depletion Eliminates Mitochondrial ADP/ATP Transport in T. brucei*—Isolated *T. brucei* mitochondria were previously shown to produce ATP in a ΔΨ-dependent manner and in the presence of ADP, free phosphate, and suitable respiratory substrates, such as succinate or α-ketoglutarate (13, 44). The efflux of mitochondrial ATP in exchange for cytosolic ADP

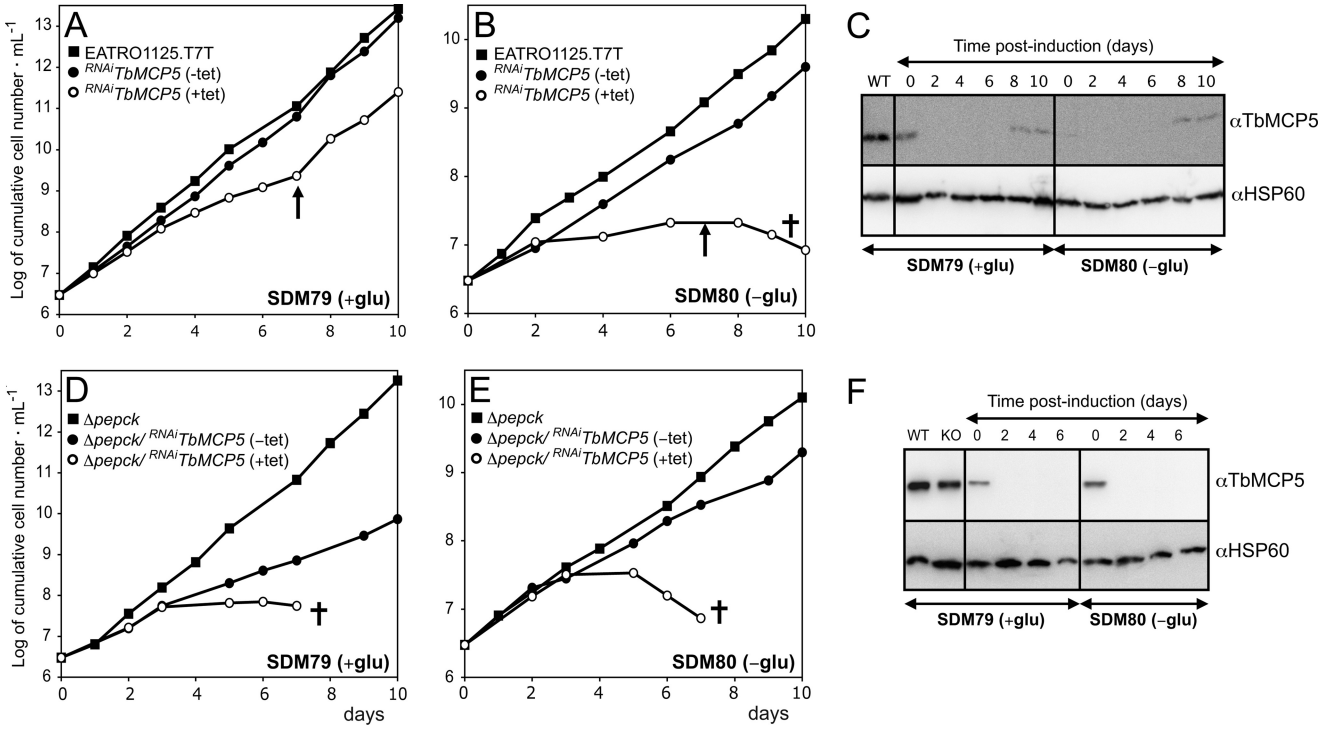


FIGURE 5. **Growth phenotype analysis of *RNAi TbMCP5* and Δ*pepck*/*RNAi TbMCP5* cell lines.** Shown are growth curves of wild type EATRO1125.T7T (*WT*) and tetracyclic-induced (+*tet*) and non-induced (−*tet*) *RNAi TbMCP5* cell lines cultured in glucose-rich SDM79 (*A*) and glucose-depleted SDM80 (*B*) culture medium. Trypanosome growth was kept exponential (between $10^6$ and $10^7$ cells $ml^{-1}$), and the shown cumulative cell numbers include normalization for dilution during cultivation. The *arrows* indicate the estimated time of TbMCP5 re-expression. *C*, Western blot analysis of wild type (WT) EATRO1125.T7T and non-induced (0 days) and tetracycline-induced (2–10 days) *RNAi TbMCP5* cell lines, using αTbMCP5 and a polyclonal *T. brucei* HSP60 antibody (αHSP60, loading control). Each lane contained $2 \times 10^6$ trypanosomes. *D–F*, like *A–C* but now with the Δ*pepck*/*RNAi TbMCP5* cell line. The Δ*pepck* double knock-out cell line is in *F*, labeled *KO*.

is in all eukaryotes exclusively catalyzed by ADP/ATP carriers (45). A mitochondrial ATP production assay (13) was used to determine whether TbMCP5 is fully or partially responsible for the mitochondrial ADP/ATP exchange in *T. brucei*. Mitochondrial ATP production was determined for the conditional Δ*TbMCP5/TbMCP5-nmyc*$^{ti}$ cell line, grown for 72 h in the presence (TbMCP5-nmyc expression) or absence (no TbMCP5-nmyc expression) of tetracycline. Mitochondria isolated from wild type PCF trypanosomes were used as control. Comparison revealed a major reduction (>90%) in mitochondrial ATP production for the TbMCP5-nmyc-depleted cell line at 72 h, when using succinate or α-ketoglutarate as mitochondrial substrates (Fig. 6*A*). Expression of TbMCP5-nmyc upon the addition of tetracycline restored the mitochondrial ATP production to wild type levels (Fig. 6*A*). These results indicated that TbMCP5 is responsible for the observed ADP/ATP exchange activity in *T. brucei* mitochondria and that the recombinant version of TbMCP5, here TbMCP5-nmyc, can functionally complement the lack of native TbMCP5. The addition of the specific ADP/ATP carrier inhibitor CATR completely eliminated mitochondrial ATP production in all cell lines (Fig. 6*A*). This confirmed that in *T. brucei*, the exchange of mitochondrial ATP for cytoplasmic ADP is exclusively facilitated by ADP/ATP carrier activity. The observed ADP/ATP exchange activity (<10%, Fig. 6*A*) in the non-induced Δ*TbMCP5/TbMCP5-nmyc*$^{ti}$ cell line at 72 h is most probably catalyzed by residual TbMCP5-nmyc protein (Fig. 4*C*, *bottom*).

*Depletion of TbMCP5 and Its Effect on the PCF Energy Metabolism*—As demonstrated above, the contribution of TbMCP5 to the energy metabolism is particularly important for PCF trypanosomes grown with proline as their main substrate for ATP production. The effect of TbMCP5 depletion on the mitochondrial proline degradation pathway was analyzed by quantifying the consumption of proline and the formation of succinate and acetate under glucose-depleted conditions. The results revealed that proline consumption is 2-fold decreased in the TbMCP5-depleted cell line, whereas succinate production is 8.7-fold increased, when compared with wild type trypanosomes (Fig. 6*B*). Interestingly, a similar reduction of proline consumption and increased succinate production was also observed when changing culture conditions for wild type PCF *T. brucei* from a glucose-depleted (proline-only) SDM80 medium to a glucose-rich SDM79 medium (9, 11). Indeed, the presence of glucose in the medium was shown to have an immediate effect on the proline metabolism (9, 11). The substantial reduction in ADP/ATP exchange activity in the TbMCP5-depleted cell line (>90%; see Fig. 6*A*) most probably leads to an aberrant mitochondrial ADP/ATP ratio, with a limited availability of ADP and the accumulation of ATP in the mitochondrial matrix. This in turn reduces the activity of ADP-dependent enzymes, thereby causing ATP-dependent feedback inhibition of the electron transport chain and coupled oxidative phosphorylation. The increased production of the metabolic intermediate succinate would be the direct consequence of this inhibition.

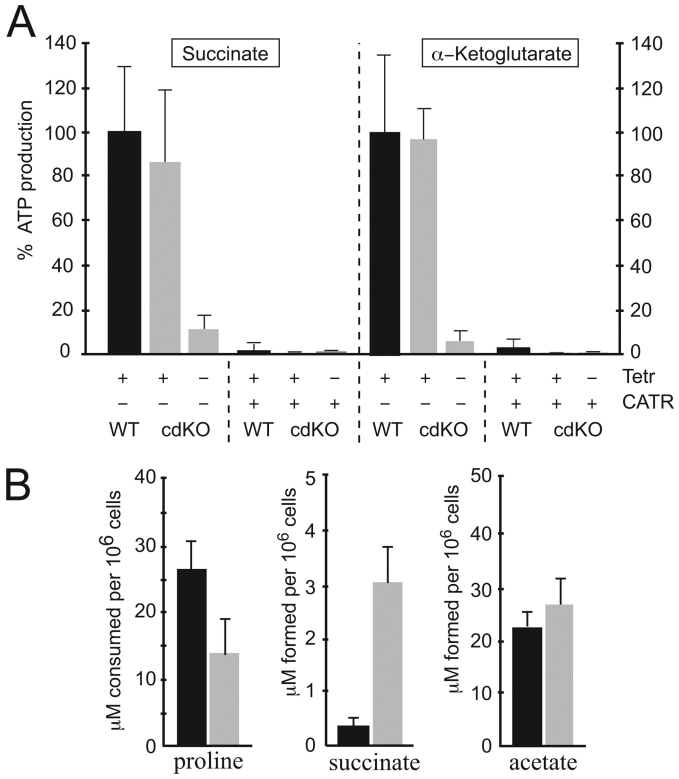


FIGURE 6. **Mitochondrial ATP production.** *A*, intact mitochondria were isolated from wild type PCF *T. brucei* (*WT*) and from non-induced (−*tet*) and tetracycline-induced (+*tet*) Δ*TbMCP5/TbMCP5-nmyc*$^{ti}$ (conditional double knock-out (*cdKO*)) trypanosomes at 72 h. Mitochondrial ATP production was initiated by the addition of succinate (*left*) or α-ketoglutarate (*right*). ATP production in WT mitochondria from succinate or α-ketoglutarate was set to 100%. Mitochondrial ATP production (export) was completely inhibited by the addition of CATR. Data shown are means of more than three independent experiments. *B*, proline consumption and product formation (succinate, acetate) for wild type and non-induced Δ*TbMCP5/TbMCP5-nmyc*$^{ti}$ (TbMCP5-depleted) PCF *T. brucei*, cultured in glucose-depleted SDM80 medium for 72 h. *Black* and *gray bars* represent substrate consumption and product formation values for wild type and TbMCP5-depleted trypanosomes, respectively. Data means are derived from more than four independent experiments. *Error bars*, S.D.

In contrast to proline and succinate, no significant differences were found in the production of acetate when comparing wild type and TbMCP5-depleted trypanosomes (Fig. 6*B*). This result is in agreement with previously published data indicating that no or very low amounts of acetate are produced from proline, whereas the degradation of threonine is the main source of acetate production under glucose-depleted conditions (9, 46). Acetate can be produced in the mitochondrion from threonine-derived acetyl-CoA via acetate:succinate CoA-transferase (ASCT)-dependent (47, 48) and by acetyl-CoA thioesterase (ACH)-dependent pathways (49). An important difference between these pathways is that ASCT, forming the ASCT/SCoAS cycle in association with succinyl-CoA synthase (SCoAS), results in the production of ATP via substrate level phosphorylation, whereas the ACH pathway does not lead to ATP production (47–49). Silencing of SCoAS expression by RNAi confirmed that acetate could be exclusively produced from threonine by ACH (49). This pathway does not result in ATP production and is thus not dependent on a functional mitochondrial ADP/ATP carrier. Our results are in agreement with this observation, because acetate production was apparently not affected by the depletion of the mitochondrial ADP/ATP carrier TbMCP5.

## DISCUSSION

Comprehensive sequence analysis and functional complementation experiments in the *ANC*-deficient *S. cerevisiae* mutant *JL1*Δ*2*Δ*3u*$^{-}$ indicated that TbMCP5 functions as a mitochondrial ADP/ATP carrier. This was further reinforced by the results from the mitochondrial ATP production assays, which revealed elimination of mitochondrial ADP/ATP exchange activity in PCF *T. brucei* upon depletion of TbMCP5. Heterologous expression in *JL1*Δ*2*Δ*3u*$^{-}$ and mitochondrial transport assays revealed that the biochemical properties and ADP/ATP exchange kinetics of TbMCP5 are similar to those of Anc2p, the prototypical ADP/ATP carrier from *S. cerevisiae*. We therefore expected that both TbMCP5 and ScAnc2p would restore growth of *JL1*Δ*2*Δ*3u*$^{-}$ on YPL medium to the same extent. However, the functional complementation of *JL1*Δ*2*Δ*3u*$^{-}$ with TbMCP5 was found to be suboptimal, with *JL-TbMCP5* having a significant higher doubling time then *JL-*ScANC2. The different $B_{max}^{ATR}$ and $V_{max}$ values (Table 1) obtained during the mitochondrial transport assays indicated that TbMCP5 was about 4-fold less abundant in yeast mitochondria than ScAnc2p, probably accounting for the reduced growth rate of *JL-TbMCP5*. One possible explanation could be the inefficient sorting of TbMCP5 to the yeast mitochondrion due to species-specific mitochondrial targeting signal requirements (50). In particular, the first 26 amino acid residues of ScAnc2p are important for efficient mitochondrial sorting in *S. cerevisiae* (51, 52). Sequence comparison (see Fig. 1*B*) confirmed that TbMCP5 contains an N-terminal extension that is shorter and not homologous to the one from ScAnc2p. A more detailed molecular analysis of the sequences required for the specific mitochondrial targeting of TMCP5, and of *T. brucei* MCF proteins in general, is currently under way.

The higher abundance of TbMCP5 in PCF *T. brucei* argues for a more prominent role of the ADP/ATP carrier in this life cycle stage of the parasite. This is supported by the targeted gene replacement and RNAi studies, which confirmed that expression of TbMCP5 is indeed essential for growth and survival of PCF *T. brucei*, particularly when depending on proline for mitochondrial ATP production. This is exemplified by the stronger growth phenotype of the TbMCP5-depleted $^{RNAi}$*TbMCP5* mutant in glucose-depleted medium. Indeed, the TbMCP5 mutant died under this culture condition, although TbMCP5 is re-expressed before cell death, whereas in the presence of glucose, re-expression of TbMCP5 immediately rescued growth (Fig. 5). This loss of expression control by the tetracycline-inducible system upon RNAi-mediated silencing is common for *T. brucei*, especially if the target gene is essential for growth/survival of the parasite (31). However, loss of expression control could not be observed when TbMCP5 is depleted on a *PEPCK* null background (Δ*pepck*/$^{RNAi}$*TbMCP5*), because the double mutant died (faster than the $^{RNAi}$*TbMCP5* single mutant) before re-expression of TbMCP5 could occur. These differences between the $^{RNAi}$*TbMCP5* and Δ*pepck*/$^{RNAi}$*TbMCP5* cell lines confirmed that the impact of TbMCP5 RNAi-mediated depletion on cell growth is more important

when proline, instead of glucose, is the main carbon source for ATP production. It was previously shown that deletion of the *PEPCK* gene in the Δ*pepck* cell line strongly affects glycolysis and leads to a metabolic shift toward proline catabolism (10). This proline dependence upon *PEPCK* deletion explains why the Δ*pepck*/$^{RNAi}$*TbMCP5* double mutant dies more rapidly regardless of the glucose concentration. The stronger growth phenotype observed for the Δ*pepck*/$^{RNAi}$*TbMCP5* cell line compared with the $^{RNAi}$*TbMCP5* cell line in the SDM80 glucose-depleted medium may be due to the residual glucose (<0.15 mM) coming from fetal calf serum, which could be used by the single mutant but not by the double mutant for energy production and thus growth. The essential role of TbMCP5 during PCF growth under glucose-depleted conditions is obviously due to the exclusively mitochondrial production of ATP through proline and threonine degradation, the contribution of the later being modest (2, 6). Indeed, in the absence of glucose, these two amino acids become the major carbon sources and are metabolized in the mitochondrion (9). Degradation of proline into alanine generates ATP by substrate level phosphorylation (via SCoAS) and several reduced cofactors, here NADH and $FADH_2$, which feed into the respiratory chain and may lead to an additional production of ATP by oxidative phosphorylation. Degradation of threonine into glycine and acetate generates ATP only via the ASCT/SCoAS cycle, in addition to NADH (2, 53). The absence of significant ATP production in the cytosol needs to be overcome by exporting ATP from the mitochondria to supply energy for anabolic pathways in the cytosol and other compartments. As expected, TbMCP5 depletion strongly affects proline catabolism by provoking a reduction of its consumption rate as well as its conversion into succinate. This is certainly a consequence of ATP accumulation and ADP depletion inside the mitochondrion, which would considerably down-regulate this pathway. However, the rate of acetate production is not affected, suggesting that catabolism of threonine, the main source of acetate in glucose-depleted conditions, is functional without ATP production. Millerioux *et al.* (49) recently showed that acetate can be produced from acetyl-CoA by two enzymes, one involved in ATP production (ASCT) and the other not (ACH), and proposed that this redundancy may be useful to modulate ATP production within this pathway. Here, we observed that when ATP production is impaired, the acetate branch is still functional, which strengthens the essential role of acetate production in the procyclic trypanosomes (54).

Two lines of evidences indicate that TbMCP5 is also essential for PCF trypanosomes grown under glucose-rich conditions; we did not succeed in deleting both TbMCP5 alleles via a conventional double knock-out approach, and depletion of TbMCP5 by RNAi leads to an important reduction of the growth rate until re-expression of the proteins after 7 days of induction (Fig. 5*A*). These results suggest that mitochondrial ADP/ATP exchange is also required under glucose-rich conditions to provide the cytosol or the mitochondrion with ATP produced in the other compartment. However, both compartments have a high capacity to produce their own ATP in glucose-rich conditions (*i.e.* glycolysis provides cytosolic ATP by phosphoglycerate kinase and pyruvate kinase, whereas $F_0/F_1$-ATP synthase and the ASCT/SCoAS cycle are essential for ATP production in the mitochondrion), as demonstrated by the lethal phenotype induced by inactivation of the $F_0/F_1$-ATP synthase on an ASCT null background (49) or in wild type PCF *T. brucei* (55). Further investigations are necessary to determine whether the cytosol or the mitochondrion requires additional ATP produced in the other subcellular compartment.

Western blot analysis revealed that in comparison with PCF *T. brucei*, substantially less but still a significant level of TbMCP5 is present in BSF trypanosomes. The current metabolic model of BSF trypanosomes excludes a role of the mitochondrion in the cellular provision of ATP (3, 4). Instead, BSF trypanosomes rely exclusively on glycolysis with a concomitant net ATP production in the cytosol of the parasite (3, 56). The BSF mitochondrion lacks a functional respiratory chain and key enzymes of the TCA cycle (57). Also, its ATP synthase level is reduced in comparison with PCF *T. brucei* (58), which argues for a less significant role of the BSF mitochondrion in cellular ATP provision. Depletion of the BSF $F_1$-ATPase $\alpha$ and $\beta$ subunits by RNA interference revealed that this enzyme is essential and plays a critical role in the maintenance of the mitochondrial membrane potential in this life cycle stage (58). This in turn implies a mitochondrial requirement for ATP and the presence of a functional ADP/ATP carrier. An alternative role for TbMCP5 in BSF trypanosomes could be the import of cytosolic glycolysis-derived ATP into the mitochondrial matrix; such import would not only support the maintenance of the mitochondrial membrane potential but would also provide energy for essential anabolic metabolism taking place in the mitochondrion (4). The physiological role of TbMCP5 as a mitochondrial ADP/ATP exchanger in BSF *T. brucei* is currently under investigation.

*Acknowledgments—We thank Cath Wadforth (University of Hull) and Pauline Morand (Université Bordeaux Segalen) for invaluable technical support.*

## REFERENCES

1. Embley, T. M., and Martin, W. (2006) Eukaryotic evolution, changes and challenges. *Nature* **440,** 623–630
2. Bringaud, F., Riviere, L., and Coustou, V. (2006) *Mol. Biochem. Parasit.* **149,** 1–9
3. Michels, P. A., Bringaud, F., Herman, M., and Hannaert, V. (2006) Metabolic functions of glycosomes in trypanosomatids. *Biochim. Biophys. Acta* **1763,** 1463–1477
4. van Hellemond, J. J., Opperdoes, F. R., and Tielens, A. G. (2005) The extraordinary mitochondrion and unusual citric acid cycle in *Trypanosoma brucei*. *Biochem. Soc. Trans.* **33,** 967–971
5. Chaudhuri, M., Ott, R. D., and Hill, G. C. (2006) Trypanosome alternative oxidase. From molecule to function. *Trends Parasitol.* **22,** 484–491
6. Bringaud, F., Barrett, M. P., and Zilberstein, D. (2012) Multiple roles of proline transport and metabolism in trypanosomatids. *Front. Biosci.* **17,** 349–374
7. van Weelden, S. W., Fast, B., Vogt, A., van der Meer, P., Saas, J., van Hellemond, J. J., Tielens, A. G., and Boshart, M. (2003) Procyclic *Trypanosoma brucei* do not use Krebs cycle activity for energy generation. *J. Biol. Chem.* **278,** 12854–12863
8. Bochud-Allemann, N., and Schneider, A. (2002) Mitochondrial substrate level phosphorylation is essential for growth of procyclic *Trypanosoma brucei*. *J. Biol. Chem.* **277,** 32849–32854
9. Lamour, N., Rivière, L., Coustou, V., Coombs, G. H., Barrett, M. P., and

Bringaud, F. (2005) Proline metabolism in procyclic *Trypanosoma brucei* is down-regulated in the presence of glucose. *J. Biol. Chem.* **280,** 11902–11910
10. Ebikeme, C., Hubert, J., Biran, M., Gouspillou, G., Morand, P., Plazolles, N., Guegan, F., Diolez, P., Franconi, J. M., Portais, J. C., and Bringaud, F. (2010) Ablation of succinate production from glucose metabolism in the procyclic trypanosomes induces metabolic switches to the glycerol 3-phosphate/dihydroxyacetone phosphate shuttle and to proline metabolism. *J. Biol. Chem.* **285,** 32312–32324
11. Coustou, V., Biran, M., Breton, M., Guegan, F., Rivière, L., Plazolles, N., Nolan, D., Barrett, M. P., Franconi, J. M., and Bringaud, F. (2008) Glucose-induced remodeling of intermediary and energy metabolism in procyclic *Trypanosoma brucei*. *J. Biol. Chem.* **283,** 16342–16354
12. Coustou, V., Besteiro, S., Rivière, L., Biran, M., Biteau, N., Franconi, J. M., Boshart, M., Baltz, T., and Bringaud, F. (2005) A mitochondrial NADH-dependent fumarate reductase involved in the production of succinate excreted by procyclic *Trypanosoma brucei*. *J. Biol. Chem.* **280,** 16559–16570
13. Schneider, A., Bouzaidi-Tiali, N., Chanez, A. L., and Bulliard, L. (2007) ATP production in isolated mitochondria of procyclic *Trypanosoma brucei*. *Methods Mol. Biol.* **372,** 379–387
14. Palmieri, F., Pierri, C. L., De Grassi, A., Nunes-Nesi, A., and Fernie, A. R. (2011) Evolution, structure and function of mitochondrial carriers. A review with new insights. *Plant J.* **66,** 161–181
15. Dahout-Gonzalez, C., Nury, H., Trézéguet, V., Lauquin, G. J., Pebay-Peyroula, E., and Brandolin, G. (2006) Molecular, functional, and pathological aspects of the mitochondrial ADP/ATP carrier. *Physiology* **21,** 242–249
16. Trézéguet, V., Pélosi, L., Lauquin, G. J., and Brandolin, G. (2008) The mitochondrial ADP/ATP carrier. Functional and structural studies in the route of elucidating pathophysiological aspects. *J. Bioenerg. Biomembr.* **40,** 435–443
17. Colasante, C., Peña Diaz, P., Clayton, C., and Voncken, F. (2009) Mitochondrial carrier family inventory of *Trypanosoma brucei brucei*. Identification, expression and subcellular localisation. *Mol. Biochem. Parasitol.* **167,** 104–117
18. Block, M. R., Lauquin, G. J., and Vignais, P. V. (1982) Interaction of 3′-*O*-(1-naphthoyl)adenosine 5′-diphosphate, a fluorescent adenosine 5′-diphosphate analogue, with the adenosine 5′-diphosphate/adenosine 5′-triphosphate carrier protein in the mitochondrial membrane. *Biochemistry* **21,** 5451–5457
19. Boulay, F., Brandolin, G., Lauquin, G. J., and Vignais, P. V. (1983) Synthesis and properties of fluorescent derivatives of atractyloside as potential probes of the mitochondrial ADP/ATP carrier protein. *Anal. Biochem.* **128,** 323–330
20. De Marcos Lousa, C., Trézéguet, V., Dianoux, A. C., Brandolin, G., and Lauquin, G. J. (2002) The human mitochondrial ADP/ATP carriers. Kinetic properties and biogenesis of wild-type and mutant proteins in the yeast *S. cerevisiae*. *Biochemistry* **41,** 14412–14420
21. Clémençon, B., Rey, M., Dianoux, A. C., Trézéguet, V., Lauquin, G. J., Brandolin, G., and Pelosi, L. (2008) Structure-function relationships of the C-terminal end of the *Saccharomyces cerevisiae* ADP/ATP carrier isoform 2. *J. Biol. Chem.* **283,** 11218–11225
22. Daum, G., Böhni, P. C., and Schatz, G. (1982) Import of proteins into mitochondria. Cytochrome $b_2$ and cytochrome *c* peroxidase are located in the intermembrane space of yeast mitochondria. *J. Biol. Chem.* **257,** 13028–13033
23. Dassa, E. P., Dahout-Gonzalez, C., Dianoux, A. C., and Brandolin, G. (2005) Functional characterization and purification of a *Saccharomyces cerevisiae* ADP/ATP carrier-iso 1 cytochrome *c* fusion protein. *Protein Expr. Purif.* **40,** 358–369
24. Brandolin, G., Le Saux, A., Trezeguet, V., Vignais, P. V., and Lauquin, G. J. (1993) Biochemical characterisation of the isolated Anc2 adenine nucleotide carrier from *Saccharomyces cerevisiae* mitochondria. *Biochem. Biophys. Res. Commun.* **192,** 143–150
25. Roux, P., Le Saux, A., Fiore, C., Schwimmer, C., Dianoux, A. C., Trézéguet, V., Vignais, P. V., Lauquin, G. J., and Brandolin, G. (1996) Fluorometric titration of the mitochondrial ADP/ATP carrier protein in muscle homogenate with atractyloside derivatives. *Anal. Biochem.* **234,** 31–37
26. David, C., Arnou, B., Sanchez, J. F., Pelosi, L., Brandolin, G., Lauquin, G. J., and Trézéguet, V. (2008) Two residues of a conserved aromatic ladder of the mitochondrial ADP/ATP carrier are crucial to nucleotide transport. *Biochemistry* **47,** 13223–13231
27. Hirumi, H., and Hirumi, K. (1989) Continuous cultivation of *Trypanosoma brucei* blood stream forms in a medium containing a low concentration of serum protein without feeder cell layers. *J. Parasitol.* **75,** 985–989
28. Brun, R., and Schönenberger (1979) Cultivation and *in vitro* cloning or procyclic culture forms of *Trypanosoma brucei* in a semi-defined medium. Short communication. *Acta Trop.* **36,** 289–292
29. Biebinger, S., Wirtz, L. E., Lorenz, P., and Clayton, C. (1997) Vectors for inducible expression of toxic gene products in bloodstream and procyclic *Trypanosoma brucei*. *Mol. Biochem. Parasitol.* **85,** 99–112
30. Bringaud, F., Robinson, D. R., Barradeau, S., Biteau, N., Baltz, D., and Baltz, T. (2000) Characterization and disruption of a new *Trypanosoma brucei* repetitive flagellum protein, using double-stranded RNA inhibition. *Mol. Biochem. Parasitol.* **111,** 283–297
31. Clayton, C. E. (1999) Genetic manipulation of kinetoplastida. *Parasitol. Today* **15,** 372–378
32. Bringaud, F., Peyruchaud, S., Baltz, D., Giroud, C., Simpson, L., and Baltz, T. (1995) Molecular characterization of the mitochondrial heat shock protein 60 gene from *Trypanosoma brucei*. *Mol. Biochem. Parasitol.* **74,** 119–123
33. Colasante, C., Alibu, V. P., Kirchberger, S., Tjaden, J., Clayton, C., and Voncken, F. (2006) Characterization and developmentally regulated localization of the mitochondrial carrier protein homologue MCP6 from *Trypanosoma brucei*. *Eukaryot. Cell* **5,** 1194–1205
34. Vassella, E., Straesser, K., and Boshart, M. (1997) A mitochondrion-specific dye for multicolour fluorescent imaging of *Trypanosoma brucei*. *Mol. Biochem. Parasitol.* **90,** 381–385
35. Sambrook, J., Fritsch, E. F., and Maniatis, T. (1989) *Molecular Cloning: A Laboratory Manual*, Cold Spring Harbor Laboratory, Cold Spring Harbor, New York
36. Voncken, F., van Hellemond, J. J., Pfisterer, I., Maier, A., Hillmer, S., and Clayton, C. (2003) Depletion of GIM5 causes cellular fragility, a decreased glycosome number, and reduced levels of ether-linked phospholipids in trypanosomes. *J. Biol. Chem.* **278,** 35299–35310
37. Bates, L. S., Waldren, R. P., Teare, I. D. (1973) Rapid determination of free proline for water-stress studies. *Plant Soil* **39,** 205–207
38. Bellofatto, V., and Palenchar, J. B. (2008) RNA interference as a genetic tool in trypanosomes. *Methods Mol. Biol.* **442,** 83–94
39. Wirtz, E., Leal, S., Ochatt, C., and Cross, G. A. (1999) A tightly regulated inducible expression system for conditional gene knock-outs and dominant-negative genetics in *Trypanosoma brucei*. *Mol. Biochem. Parasitol.* **99,** 89–101
40. Nury, H., Dahout-Gonzalez, C., Trezeguet, V., Lauquin, G. J., Brandolin, G., and Pebay-Peyroula, E. (2006) Relations between structure and function of the mitochondrial ADP/ATP carrier. *Annu. Rev. Biochem.* **75,** 713–741
41. Clémençon, B., Rey, M., Trézéguet, V., Forest, E., and Pelosi, L. (2011) Yeast ADP/ATP carrier isoform 2. Conformational dynamics and role of the RRRMMM signature sequence methionines. *J. Biol. Chem.* **286,** 36119–36131
42. Kunji, E. R., and Robinson, A. J. (2006) The conserved substrate binding site of mitochondrial carriers. *Biochim. Biophys. Acta* **1757,** 1237–1248
43. Babot, M., Blancard, C., Pelosi, L., Lauquin, G. J., and Trézéguet, V. (2012) The transmembrane prolines of the mitochondrial ADP/ATP carrier are involved in nucleotide binding and transport and its biogenesis. *J. Biol. Chem.* **287,** 10368–10378
44. Allemann, N., and Schneider, A. (2000) ATP production in isolated mitochondria of procyclic *Trypanosoma brucei*. *Mol. Biochem. Parasitol.* **111,** 87–94
45. Klingenberg, M. (2008) The ADP and ATP transport in mitochondria and its carrier. *Biochim. Biophys. Acta* **1778,** 1978–2021
46. Coustou, V., Besteiro, S., Biran, M., Diolez, P., Bouchaud, V., Voisin, P., Michels, P. A., Canioni, P., Baltz, T., and Bringaud, F. (2003) ATP generation in the *Trypanosoma brucei* procyclic form. Cytosolic substrate level

is essential, but not oxidative phosphorylation. *J. Biol. Chem.* **278,** 49625–49635
47. Van Hellemond, J. J., Opperdoes, F. R., and Tielens, A. G. (1998) Trypanosomatidae produce acetate via a mitochondrial acetate:succinate CoA transferase. *Proc. Natl. Acad. Sci. U.S.A.* **95,** 3036–3041
48. Rivière, L., van Weelden, S. W., Glass, P., Vegh, P., Coustou, V., Biran, M., van Hellemond, J. J., Bringaud, F., Tielens, A. G., and Boshart, M. (2004) Acetyl:succinate CoA-transferase in procyclic Trypanosoma brucei. Gene identification and role in carbohydrate metabolism. *J. Biol. Chem.* **279,** 45337–45346
49. Millerioux, Y., Morand, P., Biran, M., Mazet, M., Moreau, P., Wargnies, M., Ebikeme, C., Deramchia, K., Gales, L., Portais, J. C., Boshart, M., Franconi, J. M., and Bringaud, F. (2012) ATP synthesis-coupled and -uncoupled acetate production from acetyl-CoA by mitochondrial acetate:succinate CoA-transferase and acetyl-CoA thioesterase in *Trypanosoma*. *J. Biol. Chem.* **287,** 17186–17197
50. van Wilpe, S., Boumans, H., Lobo-Hajdu, G., Grivell, L. A., and Berden, J. A. (1999) Functional complementation analysis of yeast bc1 mutants. A study of the mitochondrial import of heterologous and hybrid proteins. *Eur. J. Biochem.* **264,** 825–832
51. Adrian, G. S., McCammon, M. T., Montgomery, D. L., and Douglas, M. G. (1986) Sequences required for delivery and localization of the ADP/ATP translocator to the mitochondrial inner membrane. *Mol. Cell Biol.* **6,** 626–634
52. Hashimoto, M., Shinohara, Y., Majima, E., Hatanaka, T., Yamazaki, N., and Terada, H. (1999) Expression of the bovine heart mitochondrial ADP/ATP carrier in yeast mitochondria. Significantly enhanced expression by replacement of the N-terminal region of the bovine carrier by the corresponding regions of the yeast carriers. *Biochim. Biophys. Acta* **1409,** 113–124
53. Bringaud, F., Ebikeme, C., and Boshart, M. (2010) Acetate and succinate production in amoebae, helminths, diplomonads, trichomonads and trypanosomatids. Common and diverse metabolic strategies used by parasitic lower eukaryotes. *Parasitology* **137,** 1315–1331
54. Rivière, L., Moreau, P., Allmann, S., Hahn, M., Biran, M., Plazolles, N., Franconi, J. M., Boshart, M., and Bringaud, F. (2009) Acetate produced in the mitochondrion is the essential precursor for lipid biosynthesis in procyclic trypanosomes. *Proc. Natl. Acad. Sci. U.S.A.* **106,** 12694–12699
55. Zíková, A., Schnaufer, A., Dalley, R. A., Panigrahi, A. K., and Stuart, K. D. (2009) The $F_0F_1$-ATP synthase complex contains novel subunits and is essential for procyclic *Trypanosoma brucei*. *PLoS Pathog.* **5,** e1000436
56. Gualdrón-López, M., Brennand, A., Hannaert, V., Quiñones, W., Cáceres, A. J., Bringaud, F., Concepción, J. L., and Michels, P. A. (2012) When, how and why glycolysis became compartmentalised in the Kinetoplastea. A new look at an ancient organelle. *Int. J. Parasitol.* **42,** 1–20
57. Priest, J. W., and Hajduk, S. L. (1994) Developmental regulation of mitochondrial biogenesis in *Trypanosoma brucei*. *J. Bioenerg. Biomembr.* **26,** 179–191
58. Brown, S. V., Hosking, P., Li, J., and Williams, N. (2006) ATP synthase is responsible for maintaining mitochondrial membrane potential in bloodstream form *Trypanosoma brucei*. *Eukaryot. Cell* **5,** 45–53